PHYSICAL REVIEW A **82**, 031401(R) (2010)

Application of multichannel quantum defect theory to unveil quantum interferences in dissociation of superexcited F_2

Xiang Gao,[1,*] Wei-Hua Zhang,[2] Yu-Xiang Mo,[2] and Jia-Ming Li[1,2]

[1]*Department of Physics, Shanghai Jiao Tong University, Shanghai 200240, China*

[2]*Department of Physics and Key Laboratory of Atomic and Molecular Nanosciences of Chinese Education Ministry, Tsinghua University, Beijing 100084, China*

(Received 24 February 2010; revised manuscript received 25 May 2010; published 8 September 2010)

We report experimental measurements of a high-precision photoreaction spectroscopy in combination with the velocity map imaging method. With such high-precision experimental measurements, we can "observe" detailed photodissociation processes of a specific superexcited state of our choosing. Based on multichannel quantum defect theory, an interesting quantum interference mechanism of dissociation of superexcited F_2 into $(F^+ + F^-)$ ion pairs has been unveiled.

DOI: 10.1103/PhysRevA.82.031401 PACS number(s): 33.80.Gj, 33.20.Ni

Molecules can be excited into superexcited states by ionizing radiation which in turn may ionize or dissociate these superexcited states into various fragments. Such superexcited molecules play important roles in radiation physics and chemistry [1] as well as in various molecular processes which are important in related scientific fields such as high-power gas laser researches [2] and astrophysical studies [3]. High-resolution xuv laser in combination with the velocity map imaging method [4–7] provides us with a new tool to study the very details of the spectroscopy and the dynamics of the molecular superexcited states. Using this method, we have measured the high-resolution photofragment yield spectra and velocity map images for F^- from the $(F^+ + F^-)$ ion pair as shown in Fig. 1. A full description of our experimental apparatus can be found in Refs. [5–7]. Briefly, the coherent xuv radiation was generated by using resonance-enhanced four-wave sum mixing in a pulsed Kr jet. A Nd-YAG (20 Hz) pumped two-dye laser system was used in the experiments. The resolution of the xuv laser was around 0.1 cm^{-1}. The F_2 gas sample was premixed with He (He, 96%; F_2, 4%), and the temperature of the supersonic-cooled F_2 beam was less than 10 K, which guarantees that the F_2 molecules were in rotational ground state. For theoretical aspects, several authors [8] have successfully used the quantum defect theory (QDT) to analyze the total photodissociation spectra of some molecules. We have studied the high-precision total F^- yield spectra in the framework of QDT [9], as shown in Fig. 1.

Based on our calculations [9], in the experimental xuv energy region (126 510–127 560 cm^{-1}), F_2 molecules are mainly photoexcited into Rydberg series $(F_2^+ {}^2\Pi_{3/2})np\pi_u$ and $(F_2^+ {}^2\Pi_{1/2})np\pi_u$, which are superexcited states dissociating into F^+ and F^- pairs via a dissociative state $\pi_u^3\pi_g^3\sigma_u^2({}^3\Sigma_u^-)$ with much larger electron-electron interaction matrix elements $\langle\pi_u^4\pi_g^3np\pi_u|\frac{1}{r_{12}}|\pi_u^3\pi_g^3\sigma_u^2\rangle$. In Fig. 1(a), we display the high-resolution total photofragment yield spectra for F^- ions together with the theoretical vibrational resolved assignments [9]. Figure 1(b) shows the calculated intensities which are in agreement with experimental observations [9]. Such an experimental method can be used to observe detailed photodissociation processes as illustrated by a schematic drawing in Fig. 2. The F_2 molecules are excited into superexcited states (Rydberg states) mainly through ${}^1\Sigma_g^+ \rightarrow {}^1\Sigma_u^+$ electric-dipole transitions. Because of spin-orbit interactions within the reaction zone, the Rydberg states have a non-negligible ${}^3\Sigma_u^-$ component. Through the interactions with the dissociative state ${}^3\Sigma_u^-$, the superexcited Rydberg states are dissociated. The amplitude in ${}^3\Sigma_u^-$ evolves into two amplitudes in ${}^3\Sigma_u^-$ and ${}^3\Pi_u$ via nonadiabatic interactions (radial and rotational couplings) [10] in a nonadiabatic coupling zone. Finally, dissociations into $(F^+ + F^-)$ ion pairs occur via quantum interferences between the ${}^3\Sigma_u^-$ and ${}^3\Pi_u$ states in the dissociation zone. For the velocity images from the ion-pair production processes, there are very interesting phenomena. More specifically, at the resonance at about 127 150 cm^{-1}, photoexcited F_2 molecules are dissociated into two kinds of ion pairs, $F^-(^1S)$ and $F^+({}^3P_2$ and ${}^3P_0)$, in an almost isotropic manner; however at the nearby resonance at about 127 156 cm^{-1}, photoexcited F_2 molecules are dissociated into three kinds of ion pairs, $F^-({}^1S)$ and $F^+({}^3P_2, {}^3P_1$, and ${}^3P_0)$, in an anisotropic manner as shown in Fig. 1. In the present article, we unveil general mechanisms for such interesting photodissociation processes, which are quantum interference phenomena in nature.

In photoabsorption processes, F_2 molecules in the ground state $(\text{core})\pi_u^4\pi_g^4\,{}^1\Sigma_g^+$ are excited into excited states consisting of $F_2^+(\text{core})\pi_u^4\pi_g^3\,{}^2\Pi_{g;1/2,3/2}$ and an excited molecular electron orbital, $p\pi_u$ or $p\sigma_u$. Note that the electronic ionization threshold of F_2 is split into $I_{3/2}$ and $I_{1/2}$ because of the spin-orbit interactions. Therefore photoabsorption processes involve not only singlet states but also triplet states analogous to Ar photoabsorption processes [11]. Let us first focus on photoexcitation processes from the F_2 ground state, ${}^1\Sigma_g^+(J_o = 0^+)$. Based on multichannel QDT [11–13], the superexcited state wave functions $(J = 1^-)$ can be expressed as superpositions of eigenchannel wave functions ψ_α characterizing the detailed dynamics in the reaction zone [11–15],

$$\Psi = \sum_\alpha \psi_\alpha A_\alpha, \tag{1}$$

where the mixing coefficients A_α can be determined by electron asymptotic boundary conditions [11–15]. More specifically, the eigenchannel wave functions ψ_α represent detailed

*seangx1231@sjtu.edu.cn, seangx1231@hotmail.com

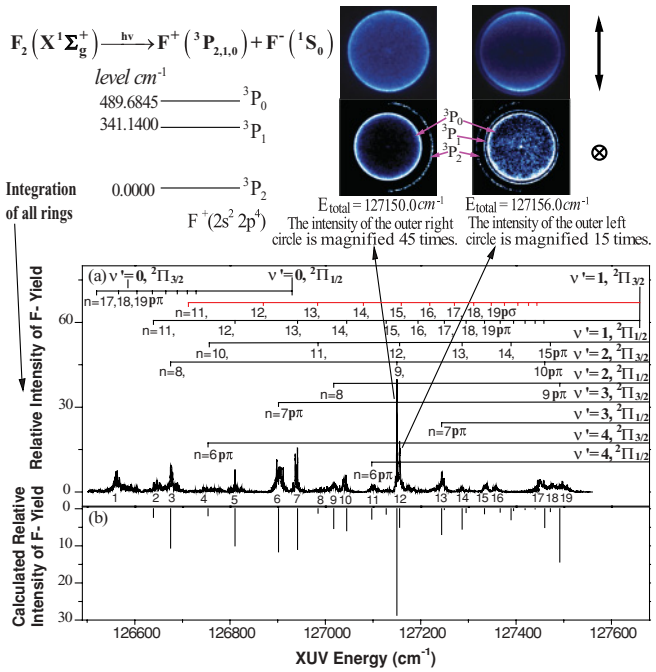

FIG. 1. (Color online) Photofragment yield spectra for F^- with velocity images in photodissociation processes into ($F^+ + F^-$) ion pairs. The four pictures are velocity images; the left two pictures are for the resonance at 127 150 cm^{-1} and the right two pictures are for the resonance at 127 156 cm^{-1}. For the upper two pictures, the laser polarization is vertical as indicated on the right. Note that the lower two pictures are magnified in order to be observed clearly with the laser polarization perpendicular to the images.

dynamical characters of an excited electron ($p\pi_u$ or $p\sigma_u$) and the molecular ionic core, $\pi_u^4\pi_g^3\,{}^2\Pi_{g,3/2,1/2}$, within the reaction zone (i.e., the molecular ion core region) denoted as Hund's Coupling Case (a) (i.e., $^{2S+1}\Lambda_\Omega$) [16] with ($J = 1^-$). There are eight eigenchannels: $^1\Sigma_{u0}^+$, $^3\Sigma_{u1}^+$, $^3\Sigma_{u0^+}^-$, $^3\Sigma_{u1}^-$, and $^3\Delta_{u1}$, arising from $p\pi_u$, and $^1\Pi_{u1}$, $^3\Pi_{u0}$, and $^3\Pi_{u1}$, arising from

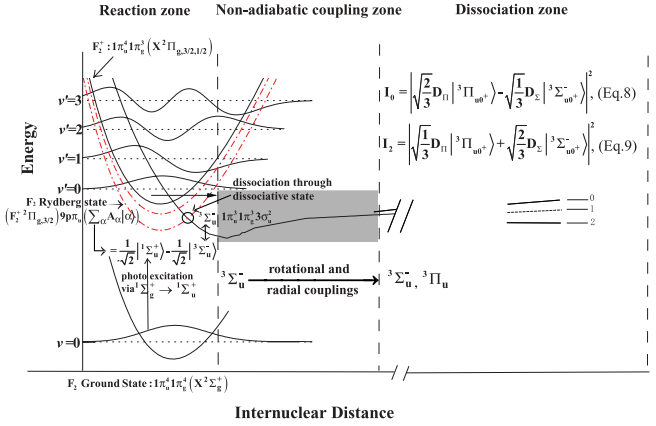

FIG. 2. (Color online) Schematic illustration of detailed processes of $F_2(X^1\Sigma_g^+) + h\nu \rightarrow F_2^{**} \rightarrow F^+(^3P_{2,1,0}) + F^-(^1S_0)$ ion-pair productions. Note that the grey shaded area involves nonadiabatic interactions among various potential curves in the nonadiabatic coupling zone and for ($F^+ + F^-$) ion-pair productions the relevant amplitudes in the $^3\Sigma_u^-$ and $^3\Pi_u$ states appear after the nonadiabatic coupling zone mainly owing to rotational couplings.

$p\sigma_u$. The eigenchannel wave functions ψ_α ($J = 1^-$) as the excited electron outside the reaction zone can also be expressed as superpositions of ionization-channel wave functions Φ_i, which are product-type wave functions of molecular ions and an excited electron [11–15] with couplings denoted as Hund's Case (e) [i.e., $^{2S_c+1}(\Lambda_c)_{\Omega_c}\,J_c(l,s)j$] [16],

$$\psi_\alpha = \sum_i U_{i\alpha}\Phi_i = \sum_i \phi_i U_{i\alpha}(f_i \cos\pi\mu_\alpha - g_i \sin\pi\mu_\alpha), \quad (2)$$

where f_i and g_i represent radial regular and irregular Coulomb wave functions of the excited electron with the common short-range phase shift $\pi\mu_\alpha$. The superposition coefficients $U_{i\alpha}$, which represent electronic and rotational interaction dynamics, that is, a transformation from Hund's Case (a) to Hund's Case (e) [17], form an orthogonal transformation matrix. The general expression of $U_{i\alpha}$ can be found in the Eq. (12) of Ref. [17]. Note that the transformation matrix **U** is very crucial in determining the important mixing coefficients A_α, as indicated in Eqs. (3) and (4) below. The ϕ_i is a combined wave function of molecular ions [$^2\Pi_{3/2}(J_c^+)$ or $^2\Pi_{1/2}(J_c^+)$] and the rotational wave function of excited electrons [$p\pi_u$ or $p\sigma_u$]. There are eight ionization channels with ($J = 1^-$); that is,

$$\begin{aligned}
&{}^2\Pi_{3/2}\left(J_c^\pi = 3/2^+\right)(l=1,s=1/2)j_u = 1/2,\\
&{}^2\Pi_{3/2}\left(J_c^\pi = 3/2^+\right)(l=1,s=1/2)j_u = 3/2,\\
&{}^2\Pi_{3/2}\left(J_c^\pi = 5/2^+\right)(1,1/2)3/2,\\
&{}^2\Pi_{1/2}\left(J_c^\pi = 1/2^+\right)(1,1/2)1/2,\\
&{}^2\Pi_{1/2}\left(J_c^\pi = 1/2^+\right)(1,1/2)3/2,\\
&{}^2\Pi_{1/2}\left(J_c^\pi = 3/2^+\right)(1,1/2)1/2,\\
&{}^2\Pi_{1/2}\left(J_c^\pi = 3/2^+\right)(1,1/2)3/2, \quad \text{and}\\
&{}^2\Pi_{1/2}\left(J_c^\pi = 5/2^+\right)(1,1/2)3/2.
\end{aligned}$$

Therefore, the molecules F_2 in the ground state $^1\Sigma_g^+(J_o^\pi = 0^+)$ are excited by xuv photons into superexcited states forming Rydberg series, $(F_2{}^+\,{}^2\Pi_{3/2})np\pi_u$ and $(F_2{}^+\,{}^2\Pi_{1/2})np\pi_u$, mainly through the $^1\Sigma_g^+ \rightarrow {}^1\Sigma_u^+$ electric-dipole transition mechanism, with the mixing coefficients A_α, which are determined by electron asymptotic boundary conditions [11–15],

$$\sum_\alpha^{N=8} U_{i\alpha}\sin\pi(\nu_{i,n}+\mu_\alpha)A_\alpha = 0, \quad \text{for all } i. \quad (3)$$

Therefore, the energy levels E_n of the Rydberg states are determined by the following equations,

$$\det|U_{i\alpha}\sin\pi(\nu_{i,n}+\mu_\alpha)| = 0, \quad (4a)$$

$$E_n = I_i - \frac{R}{\nu_{i,n}^2}, \quad \text{for all } i, \quad (4b)$$

where I_i are the ionization potentials with the Rydberg constant R. After determining the energy levels E_n (i.e., $\{\nu_{i,n}; i = 1,2,\ldots,8\}$), the corresponding A_α can be calculated by Eqs. (3) and (4) [11–15]. For the superexcited Rydberg state [$F_2{}^+\,{}^2\Pi_{3/2}(v'=2)]9p\pi_u(J^\pi = 1^-)$ at 127 150 cm^{-1}, only two of the eight A_α are dominant, namely, $A_{^1\Sigma_{u0}^+} \approx \sqrt{1/2}$ and $A_{^3\Sigma_{u0}^-} \approx -\sqrt{1/2}$. Because of the electric-dipole selection

rule from the ground state $^1\Sigma_g^+(J_o^\pi = 0^+)$ into the eigenchannel $^1\Sigma_{u0}^+$, the superexcited state, that is, the Rydberg state $[F_2{}^+\,{}^2\Pi_{3/2}(v' = 2)]9p\pi_u(J^\pi = 1^-)$ at 127 150 cm^{-1}, will be excited with the nonzero mixing coefficient $A_{^1\Sigma_{u0}^+} \approx \sqrt{1/2}$. Because of spin-orbit interactions within the reaction zone, the superexcited Rydberg state $[F_2{}^+\,{}^2\Pi_{3/2}(v' = 2)]9p\pi_u(J^\pi = 1^-)$ will have the nonzero mixing coefficient $A_{^3\Sigma_{u0^+}^-} \approx -\sqrt{1/2}$, as shown in Fig. 2, which is a key reason for dissociations into two kinds of ion pairs.

The mixing coefficient $A_{^3\Sigma_{u0^+}^-}$ is relevant to dissociations into F^+ and F^- ion pairs because of the dissociative states of the electron configuration $\pi_u^3\pi_g^3\sigma_u^2(^3\Sigma_u^-)$ with much larger interaction matrix elements $\langle\pi_u^4\pi_g^3np\pi_u{}^3\Sigma_u^-|\frac{1}{r_{12}}|\pi_u^3\pi_g^3\sigma_u^{23}\Sigma_u^-\rangle$. Through dissociation processes, the amplitudes with the initial values as $A_{^3\Sigma_{u0^+}^-}$ within the reaction zone will evolve into various amplitudes of dissociative states because of nonadiabatic interactions [10] in the nonadiabatic coupling zone (for relative small R) where nonadiabatic interactions occur among various potential curves as indicated in the grey shaded area in Fig. 2. Among them only two amplitudes, $D_{^3\Sigma_{u0^+}^-}$ and $D_{^3\Pi_{u0^+}}$, are relevant to dissociations into ion pairs, $F^-(^1S)$ and $F^+(^3P)$. Note that the nonadiabatic interactions represent the breakdown of the Born-Oppenheimer (adiabatic) approximation and involve radial couplings and rotational couplings. Especially, the rotational couplings will mix the $^3\Sigma_u^-$ and $^3\Pi_u$ states and have the following expressions of rotational-coupling potentials,

$$\begin{aligned} V_{ij}^{\mathrm{Rot}}(R) &= -\left(2\delta_{\lambda_i\lambda_{j+1}}/R^2\right)\{[(J-\Lambda_i)(J+\Lambda_i+1)]^{1/2}\langle i|iL_y|j\rangle\} \\ &\quad + \left(2\delta_{\lambda_i\lambda_{j-1}}/R^2\right)\{[(J+\Lambda_i)(J-\Lambda_i+1)]^{1/2}\langle i|iL_y|j\rangle\}. \end{aligned} \tag{5}$$

Here $|i\rangle$ and $|j\rangle$ represent $^3\Sigma_u^-$ and $^3\Pi_u$ states with the rotational-coupling matrix element $\langle i|\,iL_y\,|j\rangle$. Since the incident xuv laser is linearly polarized, the polarization direction, as indicated in the right side of the upper insert of Fig. 1, will project the molecular axis during dissociations via electric-dipole $^1\Sigma_g^+ \rightarrow {}^1\Sigma_u^+$ transition. Because the molecular rotation axis should be perpendicular to the molecular axis connecting F^+ and F^-, angular distribution will then be almost isotropic because molecular rotation averages [18] for the sharp predissociation resonance at 127 150 cm^{-1} with longer lifetime as shown in the upper-left insert of Fig. 1. Note that the molecular rotation average should be finished before reaching the dissociation zone. Furthermore, through the dissociative state $^3\Sigma_{u0^+}^-$ into the dissociation zone, only two kinds of ion pairs, that is, $F^-(^1S_0) + F^+(^3P_0)$ and $F^-(^1S_0) + F^+(^3P_2)$, will be produced, since

$$|^3\Sigma_{u0^+}^-\rangle = \sqrt{2/3}|^3P_{20}\rangle \otimes |^1S_0\rangle - \sqrt{1/3}|^3P_{00}\rangle \otimes |^1S_0\rangle, \tag{6}$$

with the molecular axis as the quantization direction throughout the present article. Similarly, through the dissociative state $^3\Pi_{u0^+}$ into the dissociation zone, only two kinds of ion pairs, that is, $F^-(^1S_0) + F^+(^3P_0)$ and $F^-(^1S_0) + F^+(^3P_2)$, will be produced, since

$$|^3\Pi_{u0^+}\rangle = \sqrt{1/3}|^3P_{20}\rangle \otimes |^1S_0\rangle + \sqrt{2/3}|^3P_{00}\rangle \otimes |^1S_0\rangle. \tag{7}$$

Therefore, as shown in Fig. 2, the intensity of dissociation into $F^-(^1S_0)$ and $F^+(^3P_0)$ ion pairs through quantum interference is

$$I_{^3P_0} = \left|\sqrt{2/3}D_{^3\Pi_{u0^+}} - \sqrt{1/3}D_{^3\Sigma_{u0^+}^-}\right|^2, \tag{8}$$

while the intensity of dissociation into $F^-(^1S_0)$ and $F^+(^3P_2)$ ion pairs through quantum interference is

$$I_{^3P_2} = \left|\sqrt{1/3}D_{^3\Pi_{u0^+}} + \sqrt{2/3}D_{^3\Sigma_{u0^+}^-}\right|^2. \tag{9}$$

Thus, with $D_{^3\Sigma_{u0^+}^-}/D_{^3\Pi_{u0^+}} \approx -0.6$, the intensity ratio $I_{^3P_0}/I_{^3P_2}$ will be about 200 at the 127 150 cm^{-1} resonance with two rings $I_{^3P_0}$ and $I_{^3P_2}$, as shown in the lower-left insert of Fig. 1.

Let us return to discuss the resonance at 127 156 cm^{-1}, as shown in the right insert in Fig. 1. The superexcited Rydberg state $[F_2{}^+\,{}^2\Pi_{1/2}(v' = 1)]12p\pi_u(J^\pi = 1^-)$ is also excited from the ground-state molecule $F_2\,{}^1\Sigma_g^+(J_o^\pi = 0^+)$ and is strongly perturbed by the Rydberg state $[F_2{}^+\,{}^2\Pi_{3/2}(v' = 1)]15p\sigma_u(J^\pi = 1^-)$ as shown in Fig. 1(a). Therefore, for the superexcited Rydberg state $[F_2{}^+\,{}^2\Pi_{1/2}(v' = 1)]12p\pi_u(J^\pi = 1^-)$, six out of the eight mixing coefficients A_α are important according to Eqs. (3) and (4), namely, $A_{^1\Sigma_{u0}^+} \approx 0.5$, $A_{^3\Sigma_{u1^-}^+} \approx 0.4$, $A_{^3\Sigma_{u0^+}^-} \approx -0.5$, $A_{^3\Sigma_{u1^-}^-} \approx 0.4$, $A_{^1\Pi_{u1}} \approx 0.3$, and $A_{^3\Pi_{u1}^-} \approx -0.3$. In addition to nonzero $A_{^3\Sigma_{u0^+}^-}$, there exists a nonzero $A_{^3\Sigma_{u1^-}^-}$, which is the key reason for dissociations into three kinds of ion pairs. Because of nonzero $A_{^1\Sigma_{u0}^+}$ and $A_{^1\Pi_{u1}}$, the superexcited Rydberg state $[F_2{}^+\,{}^2\Pi_{1/2}(v' = 1)]12p\pi_u(J^\pi = 1^-)$ is photoexcited via not only $^1\Sigma_g^+ \rightarrow {}^1\Sigma_{u0}^+$ but also via $^1\Sigma_g^+ \rightarrow {}^1\Pi_{u1}$ electric-dipole mechanisms. Because of the strong perturbation by the Rydberg state $[F_2{}^+\,{}^2\Pi_{3/2}(v' = 1)]15p\sigma_u(J^\pi = 1^-)$, in contrast to the angular distribution of two rings only, it is interesting to note that the angular distribution here is anisotropic, which indicates that the rotation averages [18] are small; that is, the lifetime of the dissociative state is short. The detailed analysis of the angular distribution of the velocity images in the whole experimental spectra has been carried out, but is beyond the scope of the present article. With the nonzero initial dissociation amplitude $A_{^3\Sigma_{u0^+}^-}$ within the reaction zone, the amplitude evolves into two relevant amplitudes $D_{^3\Sigma_{u0^+}^-}$ and $D_{^3\Pi_{u0^+}}$ because of nonadiabatic couplings [10] as shown in Fig. (2). Therefore it produces the two kinds of ion pairs, that is, $F^-(^1S_0) + F^+(^3P_0)$ and $F^-(^1S_0) + F^+(^3P_2)$, the same as the resonance at 127 150 cm^{-1} with almost the same ratio $D_{^3\Sigma_{u0^+}^-}/D_{^3\Pi_{u0^+}}$ (note that the sign is negative!). Furthermore, with the nonzero initial dissociation amplitude $A_{^3\Sigma_{u1^-}^-}$ within the reaction zone, the amplitude evolves into two relevant amplitudes $D_{^3\Sigma_{u1^-}^-}$ and $D_{^3\Pi_{u1}^-}$ via the same radial- and rotational-coupling mechanisms and the ratio $D_{^3\Sigma_{u1^-}^-}/D_{^3\Pi_{u1}^-}$ should be almost the same with the negative sign! Through the dissociative state $^3\Sigma_{u1^-}^-$ into the dissociation zone, only two kinds of ion pairs, that is, $F^-(^1S_0) + F^+(^3P_1)$ and $F^-(^1S_0) + F^+(^3P_2)$, are produced, because

$$\begin{aligned} |^3\Sigma_{u1^-}^-\rangle = 1/2|^3P_{21}\rangle|^1S_0\rangle - 1/2|^3P_{11}\rangle|^1S_0\rangle \\ -(1/2|^3P_{2-1}\rangle|^1S_0\rangle + 1/2|^3P_{1-1}\rangle|^1S_0\rangle). \end{aligned} \tag{10}$$

Similarly, through the dissociative state $^3\Pi_{u1}^-$ into the dissociation zone, only two kinds of ion pairs, that is, $F^-(^1S_0) + F^+(^3P_1)$ and $F^-(^1S_0) + F^+(^3P_2)$, are produced, because

$$|^3\Pi_{u1}^-\rangle = 1/2|^3P_{21}\rangle|^1S_0\rangle + 1/2|^3P_{11}\rangle|^1S_0\rangle - (1/2|^3P_{2-1}\rangle|^1S_0\rangle - 1/2|^3P_{1-1}\rangle|^1S_0\rangle). \quad (11)$$

Therefore, the intensity of dissociation into $F^-(^1S_0)$ and $F^+(^3P_1)$ ion pairs through quantum interference is

$$I_{^3P_1} = 1/2\left|D_{^3\Pi_{u1}^-} - D_{^3\Sigma_{u1-}^-}\right|^2, \quad (12)$$

while the intensity of dissociation into $F^-(^1S_0)$ and $F^+(^3P_2)$ ion pairs through quantum interference is

$$I_{^3P_2} = 1/2\left|D_{^3\Pi_{u1}^-} + D_{^3\Sigma_{u1-}^-}\right|^2. \quad (13)$$

With the negative ratio $D_{^3\Sigma_{u1-}^-}/D_{^3\Pi_{u1}^-}$, the intensity for the ion pairs $F^-(^1S_0) + F^+(^3P_1)$ should be larger than the intensity for the ion pairs $F^-(^1S_0) + F^+(^3P_2)$ through quantum interference. Therefore the superexcited Rydberg state $[F_2{}^+{}^2\Pi_{1/2}(v' = 1)]12p\pi_u$ will dissociate into three kinds of ion pairs with three rings, $I_{^3P_0}$(strong), $I_{^3P_1}$(medium), and $I_{^3P_2}$(weak), as shown in the lower-right insert in Fig. 1.

We would like to conclude with the following comments. Based on experimental measurements by high-precision photoreaction spectroscopy in combination with the velocity map imaging method, the detailed dissociation processes can be "observed." With such "observations," it is then possible to unveil the interesting quantum interference mechanisms of dissociations into $F^-(^1S_0) + F^+(^3P_{0,1,2})$ ion pairs for superexcited F_2 molecules within the framework of multichannel QDT [8,9,11–15]. In the experimental xuv energy region (126 510–127 560 cm^{-1}), if the F_2 molecules are pure Rydberg states $(F_2{}^+{}^2\Pi_{3/2,1/2})np\pi_u$, they will then dissociate into two kinds of ion pairs with two rings, $I_{^3P_0}$ and $I_{^3P_2}$. If the Rydberg states $(F_2{}^+{}^2\Pi_{3/2,1/2})np\pi_u$ are perturbed by $(F_2{}^+{}^2\Pi_{3/2,1/2})n'p\sigma_u$ states with the same vibrational state, they will then dissociate into three kinds of ion pairs with three rings, $I_{^3P_0}$, $I_{^3P_1}$, and $I_{^3P_2}$. The branch ratios of the rings reflect various dissociation dynamics, which may vary a lot for different superexcited states. For the two nearby resonances at about 127 150 cm^{-1} (two rings) and 127 156 cm^{-1} (three rings), although the mixing coefficients are very different, with the similar amplitude ratio of −0.6 between $D_{^3\Sigma_u^-}$ and $D_{^3\Pi_u}$, we have explained the observed velocity image branch ratios of these two states. Such measurements also provide a stringent test of accuracies with spectroscopic precision for relevant molecular collision processes. More specifically, with the physical parameters ($U_{i\alpha}$, μ_α, D, etc.) whose accuracies have been examined by such spectroscopic measurements, one can precisely calculate cross sections and reaction rates for the relevant molecular collision processes such as various electron–molecular-ion collisions including ion-pair production recombination, dissociative recombination [3,13], and molecular-ion vibrational and rotational excitation processes.

This work is supported by the Ministry of Science and Technology and the Ministry of Education of China; the Key Grant Project of the Chinese Ministry of Education (Grant No. 306020); the National Natural Science Foundation of China (Grant No. 10734040); the National High-Tech ICF Committee in China; the Yin-He Supercomputer Center, Institute of Applied Physics and Mathematics, Beijing, China; and the National Basic Research Program of China (Grant No. 2006CB921408).

[1] R. L. Plazman, Vortex **23**, 372 (1962); Radiat. Res. **17**, 419 (1962).

[2] V. V. Baranov *et al.*, JETP Lett. **39**, 515 (1984); I. V. Kholin, Quantum Electron. **33**, 129 (2003); J. P. Apruzese *et al.*, Appl. Phys. Lett. **88**, 121120 (2006).

[3] *Journal of Physics: Conference Series* 4 (2005) (Proceedings of Sixth International Conference on Dissociative Recombination: Theory, Experiments and Applications, 12–16 July 2004, Mosbach, Germany); M. Larsson and A. E. Orel, *Dissociative Recombination of Molecular Ions* (Cambridge University Press, New York, 2008).

[4] A. T. J. B. Eppink and D. H. Parker, Rev. Sci. Instrum. **68**, 3477 (1997).

[5] Y. X. Mo, J. Yang, and C. Chen, J. Chem. Phys. **120**, 1263 (2004).

[6] J. Yang, Y. S. Hao, J. Li, C. Zhou, and Y. X. Mo, J. Chem. Phys. **122**, 134308 (2005).

[7] Y. S. Hao, C. Zhou, and Y. X. Mo, J. Phys. Chem. A **109**, 5832 (2005); **111**, 10887 (2007).

[8] E. L. Hamilton and C. H. Greene, Phys. Rev. Lett. **89**, 263003 (2002); H. R. Sadeghpour, Int. J. Quantum Chem. **80**, 958 (2000).

[9] W. H. Zhang, C. L. He, Y. S. Hao, Y. X. Mo, and J. M. Li, Chin. Phys. Lett. **24**, 1220 (2007); Acta Phys. Sin. **58**, 2328 (2009) [in Chinese].

[10] A. R. Turner, D. L. Cooper, J. G. Wang, and P. C. Stancil, Phys. Rev. A **68**, 012704 (2003); C. H. Liu, Y. Z. Qu, L. Liu, J. G. Wang, Y. Li, H. P. Liebermann, P. Funke, and R. J. Buenker, *ibid.* **78**, 024703 (2008); B. H. Bransden and M. R. C. McDowell, *Charge Exchange and the Theory of Ion-Atom Collisions* (Clarendon Press, Oxford, 1992).

[11] C. M. Lee and K. T. Lu, Phys. Rev. A **8**, 1241 (1973).

[12] U. Fano, Phys. Rev. A **2**, 353 (1970); M. J. Seaton, Rep. Prog. Phys. **46**, 167 (1983); C. H. Greene and Ch. Jungen, Adv. At. Mol. Phys. **21**, 51 (1985).

[13] C. M. Lee, Phys. Rev. A **16**, 109 (1977).

[14] W. Huang, Y. Zou, X. M. Tong, and J. M. Li, Phys. Rev. A **52**, 2770 (1995); Y. Zou, X. M. Tong, and J. M. Li, Acta Phys. Sin. **44**, 50 (1995) [in Chinese].

[15] M. Aymar, C. H. Greene, and E. Luc-Koenig, Rev. Mod. Phys. **68**, 1015 (1996).

[16] G. Herzberg, *Molecular Spectra and Molecular Structure. I. Spectra of Diatomic Molecules*, 2nd ed. (Van Nostrand, Princeton, NJ, 1965); R. S. Mulliken, Rev. Mod. Phys. **2**, 60 (1930).

[17] Ch. Jungen and G. Raseev, Phys. Rev. A **57**, 2407 (1998).

[18] C. Jonah, J. Chem. Phys. **55**, 1915 (1971); S. Yang and R. Bersohn, *ibid.* **61**, 4400 (1974).